Non-symmetrical luminescent 1,2,4-oxadiazole-based liquid crystals

Hugo Gallardo[a]; Rodrigo Cristiano[a]; André A. Vieira[a]; Ricardo A. W. Neves Filho[b]; Rajendra M. Srivastava[b]; Ivan H. Bechtold[c]

[a] Departamento de Química, Universidade Federal de Santa Catarina, Florianópolis, SC - 88040-900, Brazil [b] Departamento de Química Fundamental, Universidade Federal de Pernambuco, Recife, PE - 50740540, Brazil [c] Departamento de Física, Universidade Federal de Santa Catarina, Florianópolis, SC - 88040-900, Brazil

PLEASE SCROLL DOWN FOR ARTICLE

Non-symmetrical luminescent 1,2,4-oxadiazole-based liquid crystals

Hugo Gallardo[a]*, Rodrigo Cristiano[a], André A. Vieira[a], Ricardo A. W. Neves Filho[b], Rajendra M. Srivastava[b] and Ivan H. Bechtold[c]

[a]*Departamento de Química, Universidade Federal de Santa Catarina, Florianópolis, SC – 88040-900, Brazil;* [b]*Departamento de Química Fundamental, Universidade Federal de Pernambuco, Recife, PE – 50740540, Brazil;* [c]*Departamento de Física, Universidade Federal de Santa Catarina, Florianópolis, SC – 88040-900, Brazil*

Thermal and optical behaviours of a series of highly π-conjugated hockey stick-shaped non-symmetrical 1,2,4-oxadiazoles, with liquid crystalline properties, have been studied. All of them presented liquid crystalline phases, in particular smectic and nematic phases typical of calamitic compounds. Although these substances are thermally less stable than their 1,3,4-oxadiazole isomers, they showed better liquid crystalline behaviour with lower melting points. UV–visible spectra of compounds 1a–1f in solution displayed similar absorption patterns with maxima around 320 and 350 nm ($\varepsilon \sim 2.0$–$6.0 \times 10^4 \, \text{L mol}^{-1} \text{cm}^{-1}$). All compounds exhibited strong blue fluorescence ($\lambda_{em}^{max} = 405$–468 nm) with large Stokes shift (79–117 nm). The quantum yields (Φ_F) are 42–65%, except for compounds 1c and 1f where the yields are 2 and 14%, respectively. These compounds also exhibited blue emission in the solid phase ($\lambda_{em}^{max} = 408$–492 nm).

Keywords: 1,2,4-oxadiazoles; fluorescent LCs; highly π-conjugated molecules

1. Introduction

Incorporation of heterocyclic moieties as core units in thermotropic liquid crystals can result in large changes in their mesophases and physical properties because they possess more polarisable heteroatoms, such as nitrogen, oxygen and sulfur atoms (*1*). Interest in highly π-conjugated liquid crystal molecules containing heterocycles (*2–4*) has increased enormously in the past decade due to the possibility of their use in organic light-emitting diodes (OLEDs) (*5*), where electron-deficient heteroaromatic rings can potentially offer a good charge-transporting property allied with its inherent self-organisation ability, and strong fluorescence. Compounds containing the 1,3,4-oxadiazole moiety are excellent electron-accepting materials (*6*), which have been employed as core units in calamitic (*7*) and discotic liquid crystals, which exhibited columnar mesomorphism (*8*). Depending upon the substituents at C-1 and C-5 of the 1,3,4-oxadiazole ring, these compounds may produce a bent- or hockey-stick-shaped liquid crystal with fluorescent properties (*9*). Recently, Görtz *et al.* reported the formation of chiral domains characterised by the generation of a helical macrostructure in the nematic phase of compounds containing 1,3,4-oxadiazole ring (*10*). Although, the 1,2,4-oxadiazole ring has similar properties as its 1,3,4-isomer (good luminescence and high thermal stability), liquid crystals containing 1,2,4-oxadiazole moiety have not been studied extensively (*11*). Because of the asymmetric ring, the strong lateral dipole between oxygen and nitrogen atoms leads to liquid crystalline phases different than those produced by their 1,3,4-isomers. In this context, we recently published (*12*) an efficient method for the synthesis of non-symmetrical liquid crystals based on the core 3,5-disubstituted-1,2,4-oxadiazole bearing a π-extended aromatic portion through a carbon–carbon triple bond (**1a–1f**) (Figure 1). Besides increasing the π-conjugation, the carbon–carbon triple bond in a liquid crystal molecule can also proportionately lead to a large birefringence (*13*). The aromatic groups (phenyl, naphthyl, phenylpiperazine or phenylcarboxylate) were chosen to extend the rod-shaped liquid crystal molecules, which changes their length to width ratio, and also the extended π-conjugated system, with strong electron-donating and withdrawing substituents. In continuation of our work with π-extended heterocycle-based mesogens, we report, in this paper, the entire set of thermal and optical properties exhibited by these new 1,2,4-oxadiazole liquid crystals.

2. Results and discussion

Mesomorphic properties

All compounds exhibited liquid crystalline phases, in particular the smectic C (SmC) phase, which appeared in all the structures (Figure 2). The transition temperatures, phase assignments and enthalpy

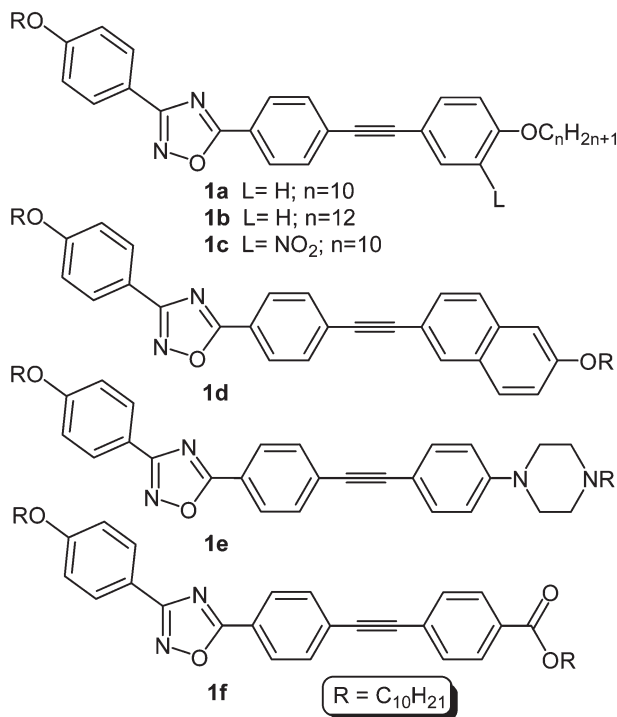*Corresponding author. Email: hugo@qmc.ufsc.br

Figure 1. Chemical structures of the studied 1,2,4-oxadiazole LCs.

energies for the materials were investigated by thermal polarising optical microscopy (POM) and differential scanning calorimetry (DSC). The optical observations were performed using clean untreated glass slides. The results are presented in Table 1.

In contrast to the results found in 1,3,4-oxadiazoles (*9a*), on increasing the terminal alkyl chain length from 10 to 12 atoms in 1,2,4-oxadiazoles **1a** and **1b** both the SmC and nematic (N) phase ranges in **1b** are decreased when compared to **1a**. The N and

Figure 2. Bar graph showing a comparative mesomorphic profile of compounds **1a–1f**.

SmC phases in these compounds were characterised by the observation of a typical Schlieren texture. Upon cooling, the Schlieren N texture changes slowly to Schlieren SmC with a clearly visible fingerprint region between the two phases, characterising a N–SmC transition. In addition, compounds **1a**, **1b**, **1d** and **1f**, exhibiting dimorphism, showed notable homeotropic behaviour of the N phase at temperatures just above the SmC–N transition. As shown in Figures 3a–3c, the optical textures on cooling sample **1d** show a Schlieren texture of the N phase at 210°C, that became dark at 204°C. On further cooling, the texture became again anisotropic and then passes to the Schlieren texture of the SmC phase at 203°C. Upon heating, the same phenomenon was observed.

Compounds **1c** and **1e**, containing a lateral nitro group and a phenylpiperazine unit, respectively, showed only smectogenic mesomorphism, i.e. smectic A (SmA) and SmC phases. The focal conic fan texture exhibited by both of these compounds (see Figure 3(d)) confirmed the SmA phase. The lateral nitro group in the extremity of **1c** clearly leads to the lowest melting point and to the absence of N phase. This was also previously observed for its 1,3,4-isomer (*9a*), and may be due to the lateral interactions of the polar groups that favour layered phases. Liquid crystals containing phenylpiperazine units have also been found to have a preference for smectic phases (*9b, 14*). This trend may be due to the polarity and
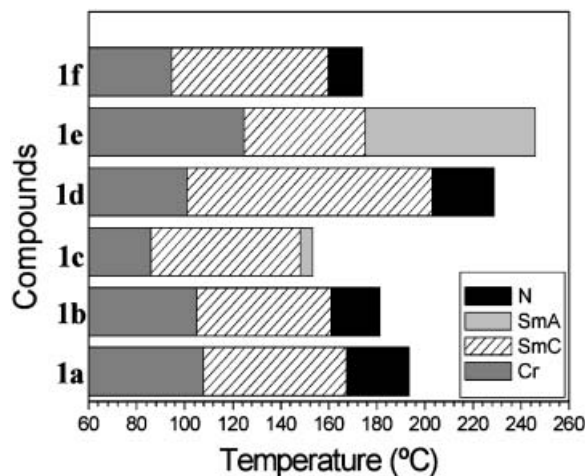
Table 1. Thermal behaviour of compounds **1a–1f**.

Compound	Transition	$T/°C$, heating ($\Delta H/$ kJ mol^{-1})[a]	$T/°C$, cooling ($\Delta H/$ kJ mol^{-1})[a]	$T_{dec.}/°C$[b]
1a	Cr–SmC	107.8 (58.5)	80.2 (−25.6)	325
	SmC–N	167.5 (0.42)	165.3 (−0.57)	
	N–I	193.4 (1.56)	192.4 (−1.75)	
1b	Cr(I)–Cr(II)	90.9 (24.8)		314
	Cr(II)–SmC	105.0 (2.46)	81.1 (−26.3)	
	SmC–N	161.1 (0.80)	158.9 (−0.81)	
	N–I	181.3 (1.50)	177.2 (−1.60)	
1c	Cr–SmC	86.0 (36.4)	59.4 (−37.0)	295
	SmC–SmA	148.1 (broad)	145.1 (broad)	
	SmA–I	153.3 (2.22)	148.9 (−2.30)	
1d	Cr–SmC	101.1 (57.8)	81.4 (−42.1)	337
	SmC–N	202.9 (0.97)	202.5 (−0.67)	
	N–I	228.8 (1.39)	225.6 (−1.13)	
1e	Cr(I)–Cr(II)	104.9 (5.47)	–	246
	Cr(II)–SmC	124.7 (2.44)	–	
	SmC–SmA	175.2 (3.56)	–	
	SmA–Dec.	246	–	
1f	Cr–SmC	94.7 (14.8)	89.9 (−9.10)	305
	SmC–N	159.7 (0.96)	145.6 (−1.60)	
	N–I	174.0 (0.08)	169.6 (−0.11)	

[a]Determined by optical microscopy and DSC measurements (10°C min^{-1}). [b]Determined by TGA, onset of decomposition in nitrogen (20°C min^{-1}).
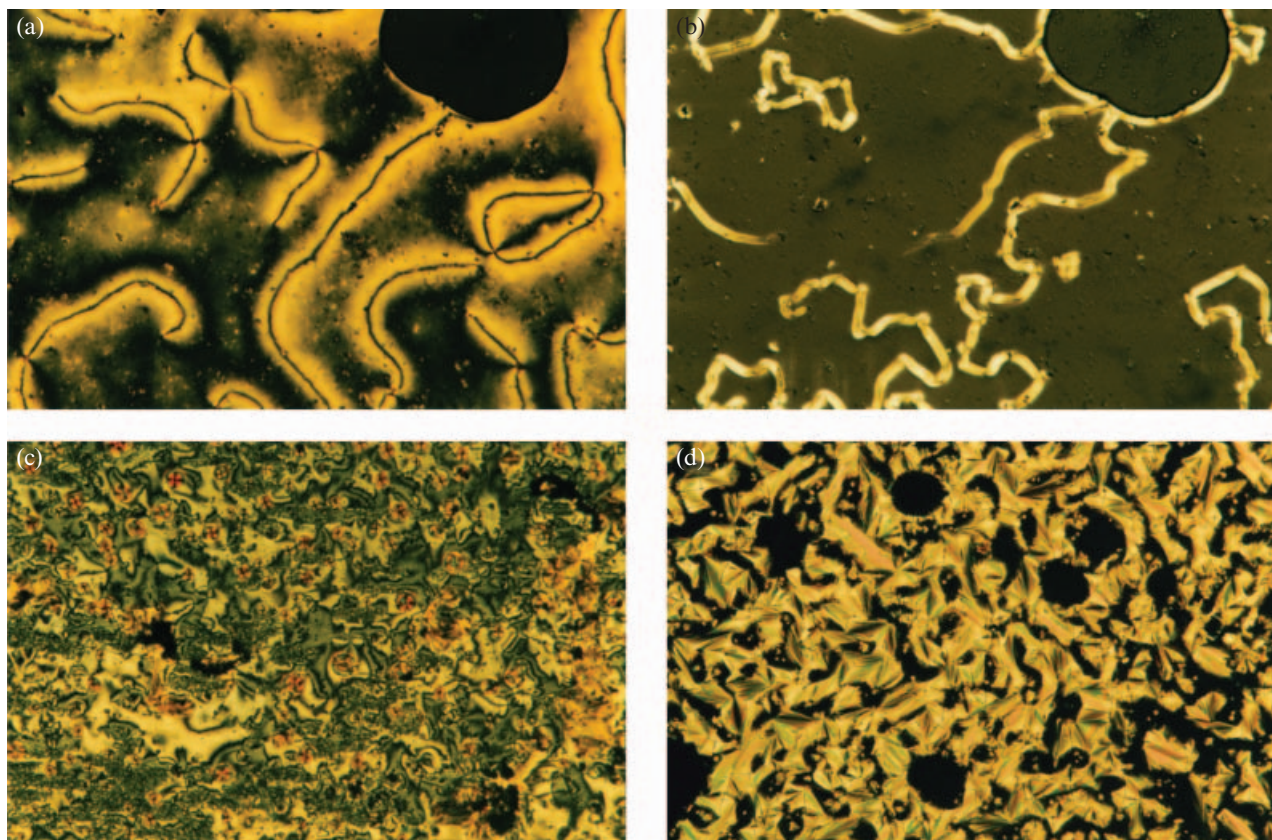

Figure 3. Photomicrographs of (a) Schlieren texture of N phase at 210°C, (b) homeotropic texture of N phase at 203°C and (c) Schlieren texture of SmC phase at 182°C, all exhibited by **1d**. (d) Focal-conic fan texture of SmA phase shown by **1c** at 151°C.

polarisability of the molecular backbone, increased by charge transfer between the lone pair on the nitrogen atom of the piperazine ring and the electron-accepting oxadiazole ring (*15*). Although compound **1e** exhibited a wide range of mesomorphism, thermal decomposition occurs at 246°C before it becomes an isotropic (I) liquid. In general, the studied compounds exhibited lower thermal stability compared to their 1,3,4-isomers, with decomposition starting about 300°C. However, most of the studied 1,2,4-oxadiazole liquid crystals showed a wide temperature range of mesophase with lower melting points.

Optical properties

The UV absorption and fluorescence spectroscopic data of 1,2,4-oxadiazole derivatives **1a–1f** in chloroform and in the solid phase are summarised in Table 2. All compounds exhibited similar absorptions between 300 and 350 nm, having maxima around 320 and 350 nm (Figure 4(a)).

These absorption bands are assigned to π–π* transitions due to their high molar absorption coefficients (ε = 2.0–6.0 × 10^4 L mol^{-1} cm^{-1}). Compounds **1c** and **1f**, which possess electron-withdrawing groups, exhibited a hypsochromic shift of 12 nm compared to 333 nm exhibited by **1a** and **1b**. Further, both these compounds displayed a shoulder around 343 nm. The increase of conjugation in the π-extended portion in **1d** led to a bathochromic shift of 12 nm in the absorption spectrum. The absorption maximum of compound **1e** was red-shifted by almost 20 nm compared to **1a** and **1b**. This could be due to an electronic effect, which lowers the LUMO–HOMO band gap due to the presence of a strong electron-donating substituent like the –NR$_2$ group (piperazine in **1e**) or -OR group together with an extended conjugation (as in **1d**). The opposite occurs in compound **1c** and **1f** (blue-shift) because of the presence of electron-withdrawing groups. The same effect is also observed in the fluorescence spectra of compounds **1a–1f** (Figure 4(b)). These compounds

exhibited blue fluorescence in solution (λ_{em}^{max} = 400–470 nm) with large Stokes shift (79–117 nm). Compounds **1a**, **1b** and **1d** produced strong fluorescence with quantum yields (Φ_F) of about 65 % relative to the quinine sulfate standard (Φ_F = 54.6 %). However, they are a slightly less fluorescent compared to their 1,3,4-oxadiazole isomers ($\Phi_F \sim 80\%$) (*9b*). Similar to its the absorption spectrum (Figure 4(a)), compound **1e** also exhibited the highest emission peak at 468 nm and the largest Stoke shift of 117 nm. This is expected to arise from a push–pull system (*16*) between a strong electron-donating group (-NR$_2$) and a strong electron-withdrawing group (oxadiazole ring). Nevertheless, this compound showed a lower photoluminescence quantum yield (Φ_F = 42.3%). This may be attributed mainly to excitation $n \rightarrow \pi$* transition from the piperazine ring that quenches the $\pi \rightarrow \pi$* excitation of the π-extended aromatic portion. Some similar quenching by the nitro and carbonyl groups occur in the emission spectra of **1c** and **1f**, respectively, due to their lower quantum yields.

All the compounds also exhibited fluorescence in the solid state. Optical absorption and emission of these materials in the solid state were measured in thin films, obtained by spin coating from chloroform solution onto a quartz plate. The solid state optical absorption and emission spectra of compounds **1a–1f** are shown in Figure 5. All lowest energy absorption bands were red-shifted in comparison to their absorption in solution. A shoulder also appeared in all of them. There were no significant changes in the fluorescence spectra of compounds **1a**, **1b** and **1d**. Interestingly, compounds with electron-withdrawing groups, such as **1c** and **1f**, exhibited a slight red-shift in their fluorescence spectra in the solid phase compared to the emission spectra in solution. In the solid phase, compound **1e** with phenylpiperazine unit showed the largest red-shift in the fluorescence spectrum. This red-shift in the electronic spectrum in solid films, compared to that in solution, is quite common for some organic dyes and has been reported by Cristiano *et al.* (*17*).

Table 2. Summary of optical properties of compounds **1a–1f**.

Compound	λ_{abs}^{max}/nm[a] (ε/10^4)[b]	λ_{em}^{max}/nm[a,c]	Stokes shift/nm	Φ_F [d]	λ_{abs}^{max}/nm[e]	λ_{em}^{max}/nm[e]	$E_g^{optical}$ [f]
1a	333 (4.7)	412	79	0.647	358	408	3.42
1b	333 (4.0)	413	80	0.652	354	408	3.44
1c	321 (4.2)	405	84	0.021	349	424	3.49
1d	345 (3.6)	437	92	0.646	358	440	3.42
1e	351 (2.2)	468	117	0.423	366	492	3.32
1f	320 (5.9)	411	91	0.140	355	422	3.45

[a]10^{-5} M in chloroform at 20°C. [b]Units = L mol^{-1} cm^{-1}. [c]Excitation wavelength was at λ_{abs}^{max}. [d]Relative quantum yield of fluorescence of quinine sulfate as standard (Φ_F = 0.546 in 1M H$_2$SO$_4$). [e]Measured in thin solid film. [f]Optical band gaps obtained from absorption spectra in solid phase.
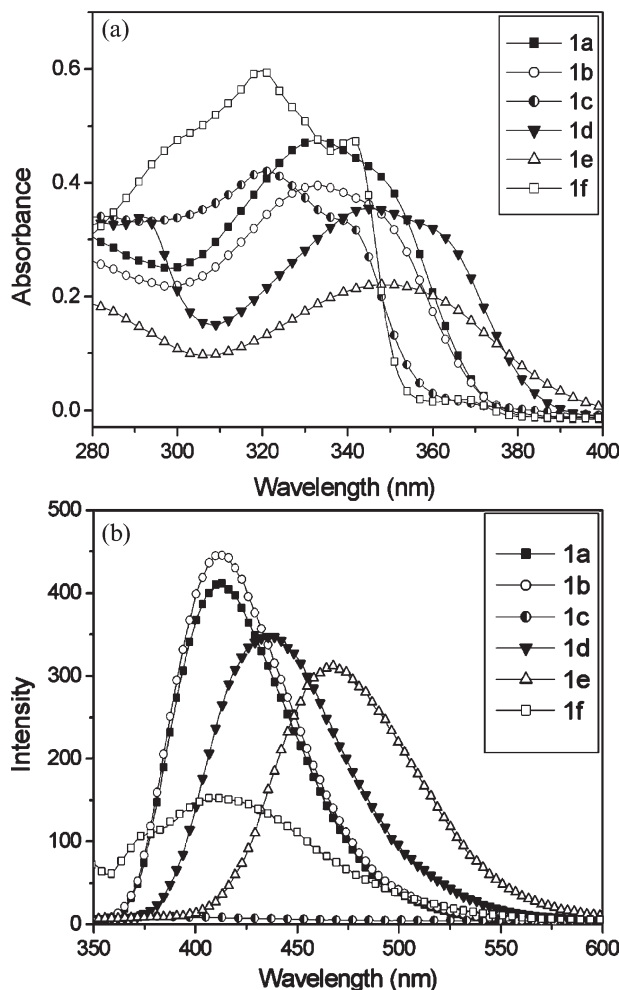
Figure 4. Absorption (a) and fluorescence (b) spectra of compounds **1a–1f** in chloroform solution.

The optical band gaps (E_g) of all compounds were determined by their corresponding absorption in thin films, using a method reported in the literature (*18*) (see Table 2). The E_g wavelengths were obtained from the derivative of the UV curves, giving the midpoint between the threshold energy at which the lowest energy absorption band starts increasing and that at which it starts decreasing. The optical band gaps of these compounds (E_g) vary from 3.32 eV in **1e** to 3.49 eV in **1c**.

3. Conclusions

In summary, the thermal and optical properties (in solution and in the solid state) of a series of non-symmetrical and luminescent 1,3,4-oxadiazole LCs were evaluated. All compounds mentioned in this work are liquid crystals exhibiting preferentially the SmC phase. Although less thermally stable than their 1,3,4-oxadiazole isomers, with decomposition temperature around 300°C, their melting points are lower and possess a wider mesophase range. These compounds displayed blue fluorescence in solution with quantum yields varying from 2 to 65% and large Stoke shifts (80 to 117 nm). In the solid state, they also present blue fluorescence with a slightly red-shifted emission peak.

4. Experimental

Materials

The materials were obtained by a convergent Sonogashira coupling reaction between building blocks of aryl iodides and the corresponding terminal aryl acetylenes using 3-(haloarylene)-5-(4-decyloxy-phenyl)-1,2,4-oxadiazole (*12*).

Equipment

The melting points, thermal transitions and meso-morphic textures were determined using an Olympus BX50 microscope equipped with a
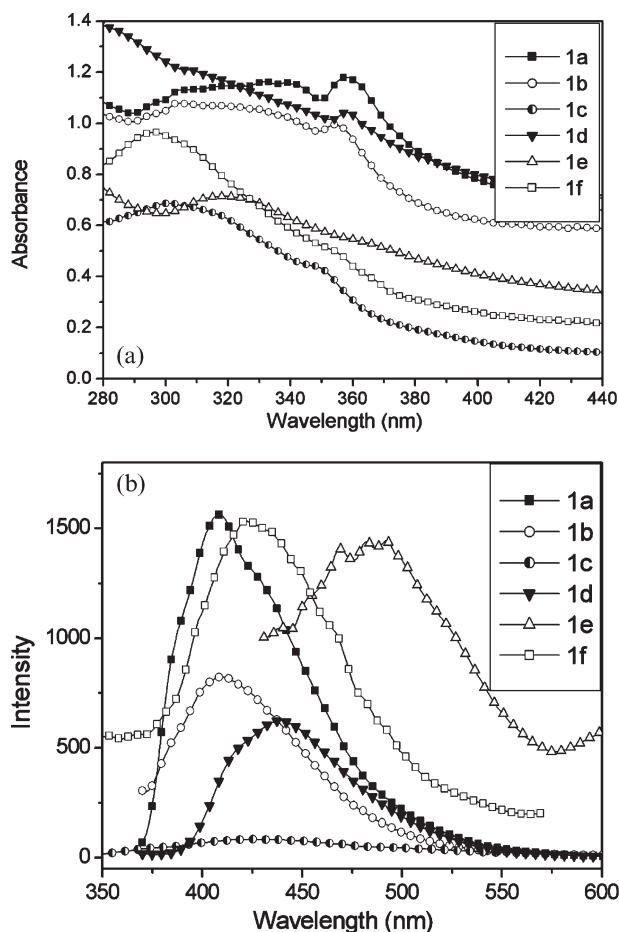
Figure 5. Absorption (a) and fluorescence (b) spectra of compounds **1a–1f** in solid phase.

Mettler Toledo FP-82 hot stage and a PM-30 exposure control unit. DSC measurements were carried out using Shimadzu equipment with a DSC-50 module. An HP UV–visible model 8453 spectrophotometer was used to record absorption spectra. Fluorescence spectra were recorded on a Hitachi-F-4500 instrument.

Fluorescence quantum yields

The relative quantum yields of fluorescence (Φ_F) for all compounds were determined according to:

$$\Phi_{unk} = \Phi_{std}(I_{unk}/A_{unk})(A_{std}/I_{std})(\eta_{std}/\eta_{unk})^2, \quad (1)$$

where Φ_{std} is the fluorescence yield of quinine sulfate standard ($\Phi_{std} = 0.546$ in 1M H_2SO_4 at 298 K), I_{unk} and I_{std} are the integrated emission intensities of the sample and the standard, respectively, A_{unk} and A_{std} are the absorbances of the sample and standard, respectively, at the desired wavelength λ_{exc} (330 nm) such that absorbance was less than 0.10, and η_{unk} and η_{std} are the refractive indexes of the sample and standard solutions.

Film preparation by spin-coating

The films were deposited on quartz plates for the optical absorption and emission measurements. Before deposition, the plates were first carefully cleaned by washing with neutral detergent and then, followed by a sequence of 20 min sonications in acetone, alcohol and water, and finally dried in an oven. The studied compounds were dissolved in chloroform, at 2 wt %, and then deposited by spin coating at 4000 rpm for 30 s at room temperature (24°C).

References

(1) (a) Seed A. *Chem. Soc. Rev.* **2007**, *36*, 2046–2069; (b) Meyer, E.; Zucco, C.; Gallardo, H. *J. Mater. Chem.* **1998**, *8,* 1351–1354; (c) Bartulín, J.; Martinez, R.; Gallardo, H.; Muller, H.; Taylor, T.R. *Mol. Cryst. Liq. Cryst.* **1993,** *225,* 175–182; (d) Gallardo, H.; Zucco, C.; Da Silva, L. *Mol. Cryst. Liq. Cryst.* **2002,** *373,* 181–190; (e) Gallardo, H.; Magnago, R.; Bortoluzzi, A.J. *Liq. Cryst.* **2001,** *28,* 1343–1352.

(2) Tokuhisa H.; Era M.; Tsutsui T. *Appl. Phys. Lett.* **1998**, *72*, 2639–2641.

(3) Attias A.-J.; Cavalli C.; Donnio B.; Guillon D.; Hapiot P.; Malthête J. *Chem. Mater.* **2002**, *14*, 375–384.

(4) (a) Vlachos P.; Mansoor B.; Aldred M.P.; O'Neill M.; Kelly S.M. *Chem. Commun.* **2005**, 2921–2931; (b) Qu, S.; Li, M. *Tetrahedron* **2007,** *63,* 12429–12436; (c) Majumdar, K.C.; Pal, N.; Debnath, P.; Rao, N.V.S. *Tetrahedron Lett.* **2007,** *48,* 6330–6333; (d) Sonntag, M.; Strohriegl, P. *Tetrahedron Lett.* **2006,** *47,* 8313–8317.

(5) (a) Shirota Y. *J. Mater. Chem.* **2000**, *10*, 1–25; (b) Apreutesei, D.; Mehl, G.H. *J. Mater. Chem. 17,* 4711–4715.

(6) (a) Adachi C.; Tsutsui T.; Saito S. *Appl. Phys. Lett.* **1989**, *55*, 1489–1491; (b) Wu, F.-I.; Shu, C.-F.; Chien, C.-H.; Tao, Y.-T. *Synth. Meth.* **2005,** *148,* 133–139; (c) Cha, S.W.; Choi, S.-H.; Kim, K.; Jin, J.-I. *J. Mater. Chem.* **2003**, *13,* 1900–1904; (d) Wang, C.; Jung, G.-Y.; Hua, Y.; Pearson, C.; Bryce, M.R.; Petty, M.C.; Batsanov, N.S.; Goeta, A.E.; Howard, J.A.K. *Chem. Mater.* **2001**, *13,* 1167–1173; (e) Xu, Z.; Li, Y.; Ma, X.; Gao, X.; Tian, H. *Tetrahedron* **2008,** *64,* 1860–1867.

(7) Sung H.-H.; Lin H.-C. *Liq. Cryst.* **2004**, *31*, 831–847.

(8) (a) Cristiano R.; Santos D.M.P.O.; Gallardo H. *Liq. Cryst.* **2005**, *32*, 7–14; (b) Wen, C.-R.; Wang, Y.-J.; Wang, H.-C.; Sheu, H.-S.; Lee, G.-H.; Lai, C.K. *Chem. Mater.* **2005,** *17,* 1646–1654; (c) Zhang, Y.-D.; Jespersen, K.G.; Kempe, M.; Kornfield, J.A.; Barlow, S.; Keppelen, B.; Marder, S.R. *Langmuir* **2003**, *19,* 6534–6536.

(9) (a) Cristiano R.; Ely F.; Gallardo H. *Liq. Cryst.* **2005**, *32*, 15–25; (b) Cristiano, R.; Vieira, A.A.; Ely, F.; Gallardo, H. *Liq. Cryst.* **2006**, *33,* 381–390.

(10) Görtz V.; Goodby J.W. *Chem. Commun.* **2005**, 3262–3264.

(11) Torgova S.; Karamysheva L.; Strigazzi A. *Braz. J. Phys.* **2002**, *32*, 593–601.

(12) Gallardo H.; Cristiano R.; Vieira A.A.; Neves Filho R.A.W.; Srivastava R.M. *Synthesis* **2008**, *4*, 605–609.

(13) (a) Wu S-.T.; Finkenzeller U.; Rieffenrath V. *J. Appl. Phys.* **1989**, *65*, 4372–4376; (b) Xianyu, H.; Gauza, S.; Song, Q.; Wu, S.-T. *Liq. Cryst.* **2007,** *34,* 1473–1478.

(14) Vieira A.A.; Cristiano R.; Bortoluzzi A.J.; Gallardo H. *J. Mol. Struct.* **2008**, *875*, 364–371.

(15) Gallardo H.; Maurmann L. *Mol. Cryst. Liq. Cryst.* **2002**, *378*, 23–34.

(16) Hohnholz D.; Schweikart K.-H.; Subramanian L.R.; Wedel A.; Wischert W.; Hanack M. *Synth. Meth.* **2000**, *110*, 141–152.

(17) Cristiano R.; Westphal E.; Bechtold I.H.; Bortoluzzi A.J.; Gallardo H. *Tetrahedron* **2007**, *63*, 2851–2858.

(18) Joshi A.; Manasreh M.O.; Davis E.A.; Weaver B.D. *Appl. Phys. Lett.* **2006**, *89*, 111907–3.